Reactive Deposition of Silicon Nanowires Templated on a Stepped Nickel Surface

Yi Wang and S. J. Sibener*

The James Franck Institute and the Department of Chemistry, The University of Chicago, 5640 S. Ellis Avenue, Chicago, Illinois 60637

The initial stages of disilane Si_2H_6 reactive deposition on Ni(977) to form silicon nanowires have been examined using scanning tunneling microscopy. The effects of disilane exposure and dosing rate on the length distributions of the resulting silicon nanowires are discussed. Creating such atomically-wide structures using reactive deposition on stepped metal templates has potential applications in "bottom-up" nanofabrication technologies, especially in the preparation of massively parallel, aligned, and high aspect ratio structures.

The controlled fabrication of nanoscale structures on surfaces is a tremendous challenge and has attracted much scientific and technological interest. As part of this endeavor, periodic features on substrates have been used as preferential nucleation sites in order to produce metallic nanowires.[1–4] At the nanometer scale, the energy spacing of the confined electronic states increases with diminishing dimension. By adjusting the confinement, it is possible to expand the energy gap between neighboring states to be larger than that of the thermal bath (*kT*). Achieving this goal will allow quantum devices and single-electron structures to be operated at room temperature.

In contrast to metallic nanoscale structures, the deposition of semiconductors on metal surfaces by vapor deposition has received limited attention.[5,6] In addition to applications in the semiconductor industry for device fabrication, semiconductor-modified metal surfaces have interesting implications in the area of catalysis since many processes are performed using metal catalysts supported on silica substrates. Moreover, electronic interactions between the semiconductor and metal support can hybridize their orbitals, leading to materials with new properties.[7–9]

In this work we have employed scanning tunneling microscopy (STM) to examine the initial stages of silicon nanowire growth by reactive deposition of disilane (Si_2H_6) on Ni(977). At low dosing exposures, Si_2H_6 decomposes on the stepped surface and forms oriented nanoscale wires which decorate the substrate's step edges. The length distribution of silicon nanowires is observed to vary as a function of total exposure and dosing rate.

Experiments were performed in a stainless steel UHV chamber with a base pressure of 5×10^{-11} Torr equipped with standard sample cleaning and characterization tools and an STM for imaging.[10] The Ni(977) surface is a 7.01° miscut of a Ni-(111) crystal in the [$2\bar{1}\bar{1}$] direction; this kinkless vicinal is composed of eight atomic row wide terraces of (111) symmetry separated by monatomic (100) step risers. Sample preparation involved cycles of 1 keV Ar$^+$ sputtering between 300 and 1100 K and annealing via electron bombardment at 1100 K. Surface cleanliness was checked by Auger electron spectroscopy and crystallinity verified using low energy electron diffraction (sharp splitting of the (111) spots) and STM. Experimental images were
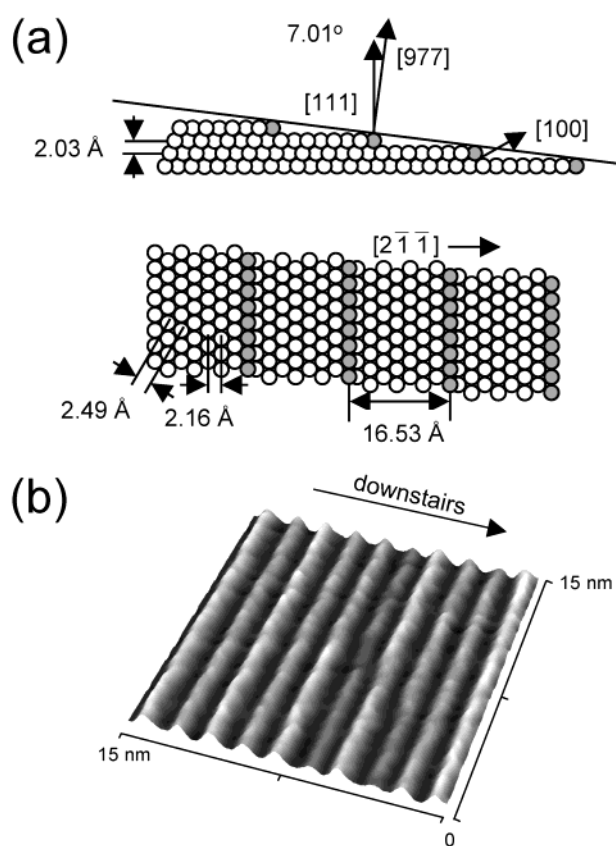
 * To whom correspondence should be addressed. E-mail: s-sibener@uchicago.edu.

Figure 1. (a) Top and side view schematic illustrations of the single step configuration for Ni(977). This surface is composed of (111) terraces, 8 atomic rows wide, separated by monatomic (100) risers. (b) STM image of a clean single-step Ni(977) surface at room temperature with a narrow terrace width distribution. The tunneling current is 1 nA with 100 mV positive sample bias. Image size is 15×15 nm^2.

recorded at room temperature in constant current mode with a tunneling current of 1 nA and a 100 mV positive bias applied to the sample. Schematic illustrations of the Ni(977) surface are shown in Figure 1 along with a corresponding STM image of a clean single-stepped region of the surface at room temperature. Disilane Si_2H_6 (0.5% in UHP Argon, Matheson) dosing was performed by chamber backfilling using a high precision leak valve. During the dosing exposure, the sample was held at a temperature of 353 K to enable disilane

Letters

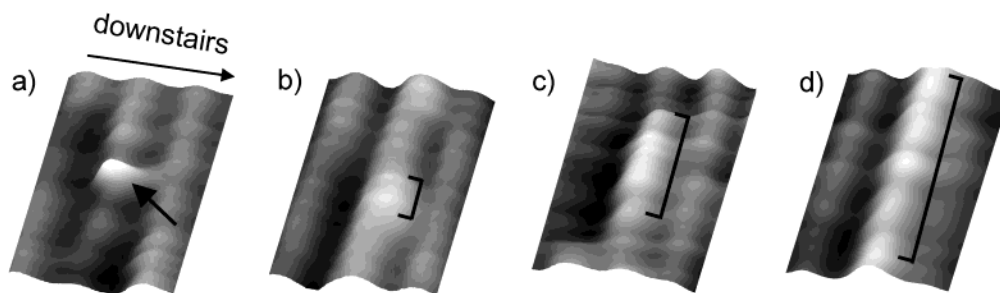*J. Phys. Chem. B, Vol. 106, No. 50, 2002* **12857**

Figure 2. Early stage growth of silicon nanowires on Ni(977). Silicon prefers to accumulate along step edges and to subsequently aggregate from initial atomic bumps (a) into more extensive nanowire structures. The tunneling current is 1 nA with 100 mV positive sample bias. Image size is 7.5 × 4.5 nm^2.
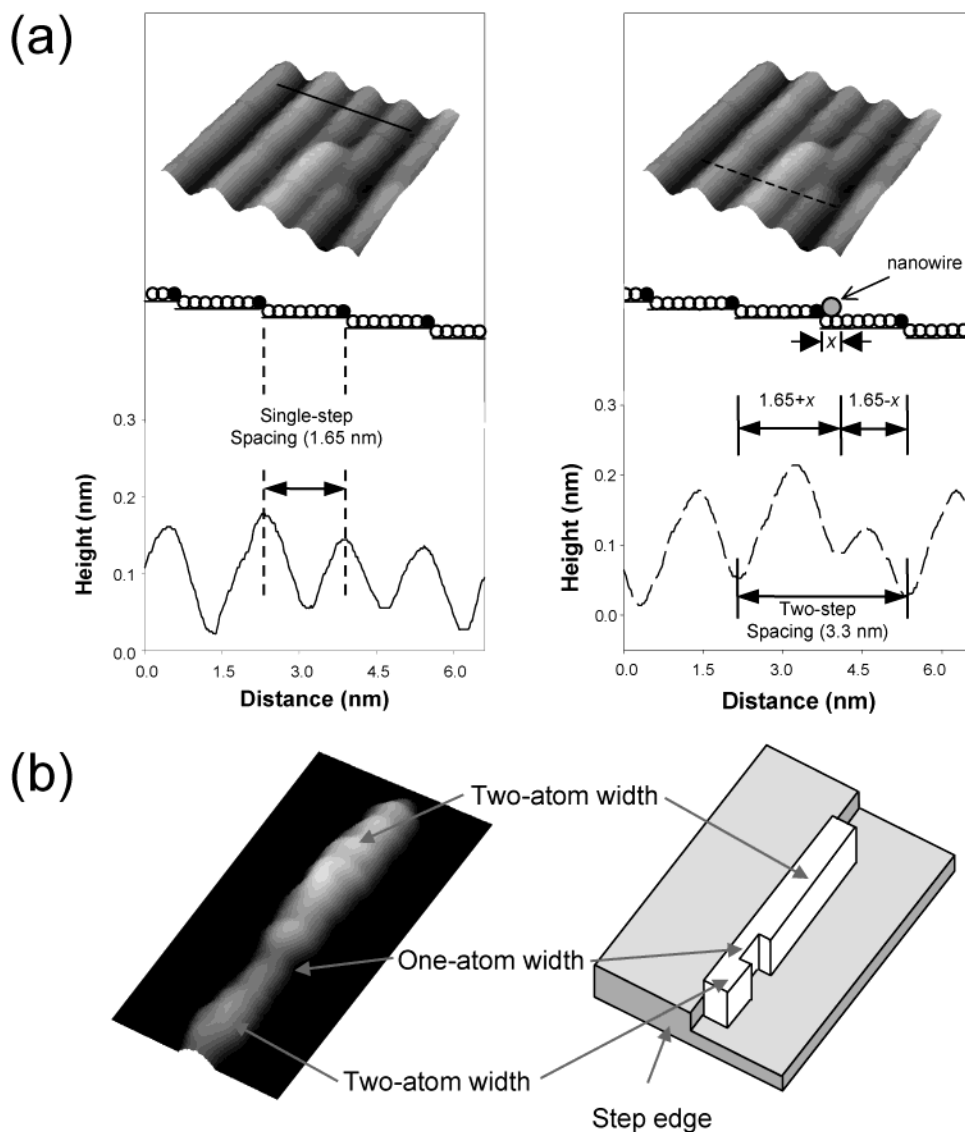

Figure 3. (a) Illustration of the method used to calculate nanowire width (x). The single terrace width is 1.65 nm. (b) STM image of a silicon nanowire with width alternating between one and two atoms. The tunneling current is 1 nA with 100 mV positive sample bias. Image size is 4 × 2 nm^2.

decomposition. The crystal was then annealed at 473 K for 10 min to desorb hydrogen. Note that the Si$_2$H$_6$ exposures reported in this paper are estimated because the 0.5% Si$_2$H$_6$/Ar mixture was highly dilute; the ion gauge sensitivity was not corrected for the differential sensitivity between Ar and Si$_2$H$_6$.

The adsorption and decomposition of silane (SiH$_4$) and disilane (Si$_2$H$_6$) on flat metal surfaces has been previously studied.[11−13] On the Ni(111) surface, SiH$_4$ decomposes at room temperature and hydrogen is largely desorbed by heating above

473 K.[13] Surface hydrogen begins to desorb around 350 K on Ni(111) and the desorption temperature of hydrogen adsorbed on Ni(977) is below 400 K.[14] Silicon will dissolve into the bulk if the temperature is above 500 K.[17] It is therefore fortuitous that a thermal window exists which allows nanowire growth before synthesis of the bulk silicide, i.e., precursor decomposition, hydrogen desorption, and Si surface diffusion occur below the 500 K dissolution temperature. Previous studies of silane decomposition on Ni(111) and polycrystalline nickel foils

suggest that the SiH_4 decomposition reaction is nucleated at surface steps and/or other surface defects because the foils are far more reactive toward SiH_4 than is the flat Ni(111) surface.[17] Similarly, on a Ni(977) surface with high step density, Si_2H_6 will likely decompose preferentially but not exclusively at step edges. We infer from the above knowledge base that with our experimental conditions Si_2H_6 decomposes and most of the hydrogen is desorbed during annealing. (Note that, because of the strong interaction between silicon and hydrogen, it is possible that SiH species exist on the surface in trace quantities even after annealing. Annealing at a higher temperature is precluded by dissolution of silicon into the bulk.) After Si_2H_6 decomposes, silicon atoms nucleate growth of nanowires. Various stages of silicon nanowire growth following exposure of Si_2H_6 are illustrated in Figure 2. The first panel demonstrates the initial formation of a single-atom silicon bump on a 7.5 nm × 4.5 nm template area, with subsequent panels showing the different growth stages of a silicon nanowire. Since we were interested specifically in early stage growth, exposures were limited such that the typical dimensions for these silicon wires were approximately 1 nm long by 0.25 nm wide; these dimensions correspond to one atom in width and 4−5 atoms in length (the atomic radius for silicon is ∼0.12 nm). Specifically, the average width of the one-atom feature is 0.27 ± 0.05 nm while that for the two-atom feature is 0.50 ± 0.06 nm. These correspond therefore, to one and two-atom wide silicon nanowires. Under higher Si_2H_6 exposures, the length of these nanowires can be increased dramatically.

The width of the line, i.e., extension away from the step edges, is calculated using the method described below (Figure 3a). STM images measure the surface electron density of states rather than the atomic geometry directly. Measuring silicon nanowire width, therefore, requires deconvolution. Clean Ni(977) STM images show uniform single-steps with widths of 1.65 nm. After decorating a step edge with silicon, the surface electron density in that local region changes dramatically. The edge-adsorbed silicon effectively increases the width of the "upstairs" terrace and equivalently decreases that of the "downstairs" terrace. It is this change which is used to estimate the silicon nanowire width using the following methodology: assume that the actual silicon nanowire width in a local region is represented by x. Recall, the total width of the two-step region is 3.3 nm (twice the single-step width) on a Ni(977) surface with low Si_2H_6 exposure (Figure 3a). The widths of these two neighboring steps can be represented by (1.65 nm + x) and (1.65 nm − x). Since the ratio of these two widths can be obtained from the experimental images, the silicon nanowire width x can be easily calculated by solving a one-variable equation.

After the initial nucleation, the wire grows gradually in two directions along the step edge (Figure 2b−d). During this process, its height remains constant; however, its width can change from one to two atoms (Figure 3b). By increasing the Si_2H_6 exposure, a larger area becomes decorated with silicon nanowires (Figure 4). Interestingly, in this intermediate regime, the increase in coverage comes with a sacrifice in average wire length. A 1.63 L Si_2H_6 exposure with a dosing rate of 0.163 L/min leads to ∼6% silicon coverage, with the average length of silicon nanowires being 6.9 nm (Figure 4a). If the Si_2H_6 exposure is increased to 16.3 L, although the total silicon coverage rises to ∼9%, the average silicon nanowire length decreases to 3.4 nm (Figure 4b). A higher dosing rate (1.63 L/min), however, leads to shorter nanowires (3.4 nm) compared with that measured (4.6 nm) using a lower dosing rate (0.815 L/min). This can be explained by the rate of nanowire
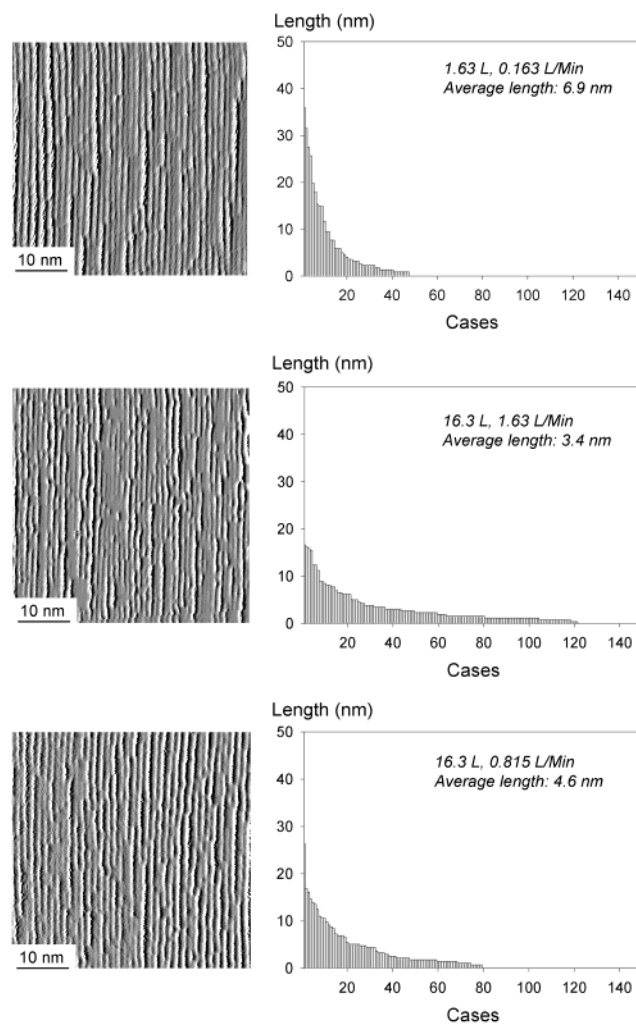

Figure 4. Different final Si nanowire distributions resulting from various Si_2H_6 dosing exposures and rates. (a) 1.63 L exposure in 10 min, (b) 16.3 L exposure in 10 min, and (c) 16.3 L exposure dosage in 20 min. The bright, linear, and aligned regions seen in all three images are the Si nanowires.

nucleation at the step edges: the experimental exposures we use are much smaller than the amount needed to fully cover all of the step edges. Hence, at higher dosing rates, more nucleation sites are formed compared to the number observed at lower rates. For a given total exposure less than that needed to fully titrate the step edges, higher dosing rates will lead to nanowires having shorter average length but with a larger number of such structures. We fully expect that using higher Si_2H_6 exposures will allow the step edges to be fully decorated and, ultimately, for the entire terraces to be completely covered by silicon.

STM has been employed to probe the reactive deposition of silicon nanowires using Si_2H_6 as the source material. Initial stages of Si_2H_6 decomposition on the stepped Ni(977) surface and the subsequent formation of silicon nanowires have been discussed. By varying the Si_2H_6 exposure and dosing rate, it is possible to form different width and length distributions of the nanowires. Moreover, recent advances in controlling the perfection of stepped structures[15] suggests that hierarchical templates of more complex structure may become available for such purposes. This method of gas-phase reactive deposition on a stepped metal surface, with the substrate acting as both catalyst and nanotemplate with easily tunable width (by varying the vicinal miscut angle) is a fruitful approach to creating massively parallel nanoscale arrays of highly aligned structures.

References and Notes

(1) Himpsel, F. J.; Ortega, J. E.; Mankey, G. J.; Willis, R. F. *Adv. Phys.* **1998**, *47*, 511−597.

(2) Lin, J. L.; Petrovykh, D. Y.; Kirakosian, A.; Rauscher, H.; Himpsel, F. J.; Dowben, P. A. *Appl. Phys. Lett.* **2001**, *78*, 829−831.

(3) Pietzsch, O.; Kubetzka, A.; Bode, M.; Wiesendanger, R. *Phys. Rev. Lett.* **2000**, *84*, 5212−5215.

(4) Pietzsch, O.; Kubetzka, A.; Bode, M.; Wiesendanger, R. *Science* **2001**, *292*, 2053−2056.

(5) Endres, F.; Zein El Abedin, S. *Phys. Chem. Chem. Phys.* **2002**, *4*, 1649−1657.

(6) Nakato, Y.; Murakoshi, K.; Imanishi, A.; Morisawa, K. *Electrochemistry* **2000**, *68*, 556−561.

(7) Kraus, A.; Erbe, A.; Blick, R. H. *Nanotechnology* **2000**, *11*, 165−168.

(8) Ko, M.-J. *Adv. Mater. Opt. Electron.* **1998**, *8*, 173−180.

(9) Caruso, R. A.; Antonietti, M.; Giersig, M.; Hentze, H.-P.; Jia, J. *Chem. Mater.* **2001**, *13*, 1114−1123.

(10) Pearl, T. P.; Sibener, S. J. *Rev. Sci. Instrum.* **2000**, *71*, 124−127.

(11) Wiegand, B. C.; Lohokare, S. P.; Nuzzo, R. G. *J. Phys. Chem.* **1993**, *97*, 11553−11562.

(12) Mccash, E. M.; Chesters, M. A.; Gardner, P.; Parker, S. F. *Surf. Sci.* **1990**, *225*, 273−280.

(13) Dubois, L. H.; Nuzzo, R. G. *Surf. Sci.* **1985**, *149*, 133−145.

(14) Hanbicki, A. T.; Darling, S. B.; Gaspar, D. J.; Sibener, S. J. *J. Chem. Phys.* **1999**, *111*, 9053−9057.

(15) Wang, Yi; Pearl, T. P.; Darling, S. B.; Gimmell, J. L.; Sibener, S. J. *J. Appl. Phys.* **2002**, *91*, 10081−10087.